Wavenumber Distribution in Hopf-Wave Instability: The Reversible Selkov Model of Glycolytic Oscillation

Arun K. Dutt*

Faculty of Computing, Engineering and Mathematical Sciences, Du Pont Building, University of the West of England, Frenchay Campus, Bristol BS16 1QY, United Kingdom, and 16, Ghanarajpur (Jalapara), Dhaniakhali, District Hooghly, West Bengal 712302, India

Received: March 17, 2005; In Final Form: June 27, 2005

We have investigated the short-wave instability due to Hopf bifurcation in a reaction−diffusion model of glycolytic oscillations. Very low values of the ratio *d* of the diffusion coefficient of the inhibitor (ATP) and that of the activator (ADP) do help to create short waves, whereas high values of the ratio *d* and the complexing reaction of the activator ADP reduces drastically the wave-instability domain, generating much longer wavelengths.

Introduction

Pattern formation in reaction−diffusion (R−D) systems has been a subject of intensive research in recent years.[1−5] However, the Hopf-wave instability with nonzero wavenumber (short wavelength instability) has received less attention particularly in the case of biochemical oscillators. The discovery of Turing structures[6] in the CIMA reaction[7] and in its variant CDIMA reaction[8−10] seems to be the result of the fortunate coincidence that starch and polyacrylamide (PAA) gel were also present in the system. Several experiments have investigated the effect of starch and the gel in this reaction. Lee et al.[11] obtained Turing structures in a PAA gel without using starch. Agladze et al.[12] obtained these structures in a gel-free aqueous solution of the CIMA reaction at a high starch concentration. In agarose gel, which does not interact chemically with iodine species, the presence of starch is necessary[12] for generating Turing structures. At low starch concentration, the system is shifted to the oscillatory state, producing travelling waves rather than Turing structures. Noszticzius et al.[13] obtained Turing structures in the CDIMA reaction using polyvinyl alcohol instead of starch as the I_3^- indicator

Epstein et al.[14,15] have suggested the hypothesis that the complexing reaction of the activator iodine species with the starch indicator or with the polyacrylamide gel results in a major reduction of the effective activator diffusion coefficient. When this hypothesis is included into their model[8,9] (LE model), one can simulate Turing structures (viz. hexagons, stripes, rhombi, etc.) in the CDIMA reaction with intrinsic wavelengths very much comparable to those obtained in experiments.

The spatio-temporal patterns in biological systems are extremely important due to their wide applications in morphogenesis. Our numerical work[16] on the reversible Selkov model,[17] a generic model of glycolytic oscillations,[18] has demonstrated how the Hopf-wave-instability domain is reduced drastically in the presence of the complexing reaction of the activator, resulting in a massive increase in the Turing domain in parameter space. In the present numerical investigation, we have reported the wavenumber distribution of Hopf-wave instability in the parameter space in this model in the absence and presence of the complexing reaction of the activator ADP.

Model

Self-oscillations in glycolysis were first discovered in intact yeast cells and yeast cell extracts and also in beef heart extract. The phosphofructokinase (PFK1) reaction is considered as being the possible source of self-oscillations in glycolysis. Selkov[18] proposed a simple kinetic model of enzyme catalysis with product activation of the enzyme, which exhibits limit-cycle oscillations. In this model, a substrate S (ATP) supplied by a certain source at a constant rate is converted irreversibly into a product P (ADP). The product P (ADP) is removed by an irreversible sink at another constant rate. The free enzyme PFK1 is inactive by itself, but becomes active after combination with product molecules (ADP) to form a complex. On the basis of Selkov's model, Richter et al.[17] proposed the following three reversible kinetic steps, known as the reversible Selkov model

$$\mathrm{A} \rightleftharpoons \mathrm{S}$$

$$\mathrm{S} + 2\mathrm{P} \rightleftharpoons 3\mathrm{P}$$

$$\mathrm{P} \rightleftharpoons \mathrm{B} \qquad \text{(I)}$$

where *A* and *B* are controllable source and sink concentrations and $k_{\pm i}$ ($i = 1, 2, 3$) are, respectively, the rate constants of the three steps. (The + and − subscripts are, respectively, for the forward and reverse reactions.) When described in terms of the activator/inhibitor model, the autocatalyst P is the activator, and S the inhibitor. When the reaction part and the diffusion part are scaled as given in eqs 1a[17] and 1b,[8,9] respectively

$$k_3 t = \tau \quad S/N = s \quad P/N = p$$

$$N = (k_3/k_2)^{1/2} \quad a = (k_1 A)/(k_3 N) \quad b = (k_{-3} B)/(k_3 N)$$

$$\kappa = (k_{-1}/k_3) \quad K_2 = (k_{-2}/k_2) \qquad \text{(1a)}$$

$$\rho = x(k_3/D_p)^{1/2} \qquad \text{(1b)}$$

* Author to whom correspondence should be addressed. Present address: 16, Ghanarajpur (Jalapara), Dhaniakhali, District Hooghly, West Bengal 712302, India. E-mail : dutt_arun@yahoo.com.

10.1021/jp058096c CCC: $30.25
Published on Web 08/27/2005

the R−D equations in one dimension take the form as given in eqs 2a and 2b

$$\partial p/\partial \tau = -p + b + sp^2 - K_2p^3 + (\partial^2 p/\partial \rho^2) \quad (2a)$$

$$\partial s/\partial \tau = a - \kappa s - sp^2 + K_2p^3 + d(\partial^2 s/\partial \rho^2) \quad (2b)$$

where A (a), P (p), and S (s) represent the concentrations (scaled concentrations) of the respective species, D's are diffusion coefficients, x is the geometrical coordinate, and

$$d = D_s/D_p \quad (3)$$

The dimensionless eqs 2a and 2b may be written in the form

$$\partial p/\partial \tau = f(p,s) + (\partial^2 p/\partial \rho^2) \quad (4a)$$

$$\partial s/\partial \tau = g(p,s) + d(\partial^2 s/\partial \rho^2) \quad (4b)$$

where $f(p,s)$ and $g(p,s)$ are the nonlinear reaction functions of the two dimensionless partial differential eqs 2a and 2b.

If the activator P is involved in a complexing reaction[15] similar to that reported in the Turing structure experiments and modeling of the CIMA oscillatory reaction, we have the chemical equilibrium as given below

$$\mathrm{P} + \mathrm{C} \rightleftharpoons \mathrm{PC} \quad (\mathrm{II})$$

where the activator P is captured partially to produce the complex PC reacting with the chemical species C. The equilibrium constant K, of this complex formation reaction is given by

$$K = (pc)/pc \quad (5)$$

where (pc), p, and c are the equilibrium concentrations of the complex PC, the activator P, and the complexing agent C, respectively. If we use the complexing agent in large excess such that the initial concentration (c_0) of the complexing agent is almost equal to its concentration (c) at chemical equilibrium, then one can define a new constant K' such that

$$K' = Kc_0 \quad (6)$$

Therefore, due to the complexing reaction of the activator P, the new R−D equations take the form as given below

$$\partial p/\partial \tau' = f(p,s) + (\partial^2 p/\partial \rho^2) \quad (7a)$$

$$\partial s/\partial \tau' = (1 + K')\,[g(p,s) + d(\partial^2 s/\partial \rho^2)] \quad (7b)$$

where

$$\tau = (1 + K')\tau' \quad (8)$$

The characteristic equation for the dimensionless partial differential eqs 7a and 7b can be written as

$$\det\begin{bmatrix} a_{11} - k^2 - \omega_k & a_{12} \\ a_{21} & a_{22} - (1 + K')k^2 d - \omega_k \end{bmatrix} = 0 \quad (9)$$

where

$$a_{11} = f_p' \quad a_{12} = f_s'$$

$$a_{21} = (1 + K')g_p' \quad a_{22} = (1 + K')g_s' \quad (10a)$$

and from eqs 2a and 2b, we have the following relations

$$f_p' = -1 + 2s_0p_0 - 3K_2{p_0}^2$$

$$f_s' = {p_0}^2$$

$$g_p' = -2s_0p_0 + 3K_2{p_0}^2$$

$$g_s' = -\kappa - {p_0}^2 \quad (10b)$$

First, we consider this two variable system for the homogeneous ($k = 0$) mode. A Hopf bifurcation of the homogeneous system occurs when for the stability matrix **A,** given by eq 11

$$\mathbf{A} = \begin{bmatrix} a_{11} & a_{12} \\ a_{21} & a_{22} \end{bmatrix} \quad (11)$$

$$\mathrm{Tr}\,\mathbf{A} = a_{11} + a_{22} = 0 \quad (12)$$

Substituting the values of a_{11} and a_{22} in eq 12 from eqs 10a and 10b, one obtains

$$\kappa(1 + K') + K'{p_0}^2 = -1 + 2s_0p_0 - 3K_2{p_0}^2 - {p_0}^2 \quad (13)$$

From the characteristic eq 9 for nonzero k-mode, the condition for Hopf bifurcation is given by

$$k^2d - a_{22} + k^2 + k^2dK' - a_{11} \le 0 \quad (14a)$$

for

$$\det\mathbf{A} - (a_{22} + da_{11} + da_{11}K')k^2 + d(1 + K')k^4 > 0 \quad (14b)$$

From eq 14a, we have

$$k^2_{\mathrm{Hopf}} \le \frac{a_{11} + a_{22}}{1 + (1 + K')d} \quad (15)$$

Results and Discussion

Hopf bifurcation of the homogeneous ($k = 0$) and inhomogeneous ($k \neq 0$) model system is strongly affected by complex formation with the activator P. The Hopf eq 13 for the homogeneous system ($k = 0$) depends very much on K', the degree of complex formation with the activator P—the Hopf boundary would be shifted to a lower value of κ if K' has values >0. This is presented in Figure 1 with two more values of K' (0.5 and 1.5).

In the case of Hopf-wave bifurcation ($k \neq 0$ mode), the wavenumber (wavelength) depends strongly on the degree (K') of the complexing reaction of the activator P. This is evident from eq 15 and also in Figures 2a and 2b, suggesting that due to the complexing reaction of the activator (K', 0.5) there is an approximately 2-fold decrease (increase) of Hopf-wavenumber (wavelength) values. The computed Hopf wavenumbers (Figure 2b) in the presence of the complexing reaction of the activator ADP have values in the range 0.02−0.1 for $d = 1$ (a reasonable value for the ratio of the diffusion coefficient of the inhibitor to that of the activator in aqueous solution). When translated to wavelength, this range becomes 314−62.8 in the dimensionless unit of ρ, which on further transformation to real length with the help of eq 1b becomes between 3 and 0.6 mm for $D_p \approx 10^{-5}$ cm^2 s^{-1} and $k_3 \approx 10$ s^{-1}. Therefore, our model calculations predict inhomogeneous Hopf waves on the order of a few millimeters in length. The work of Müller et al.,[19] which obtained polygonal network patterns (size $\approx$ 0.5−1 mm) in a

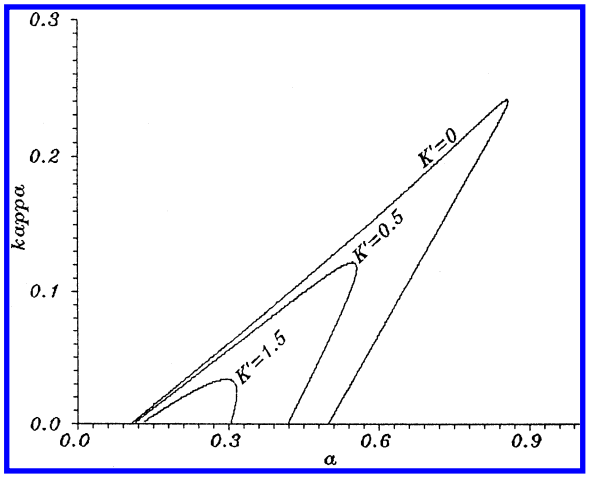

Figure 1. Phase diagram in the $a-\kappa$ phase plane of the homogeneous ($k = 0$) reversible Selkov model for $K' = 0$, 0.5, and 1.5: b, 0.09; K_2, 1; a and b are the scaled concentrations of source A and sink B, respectively.

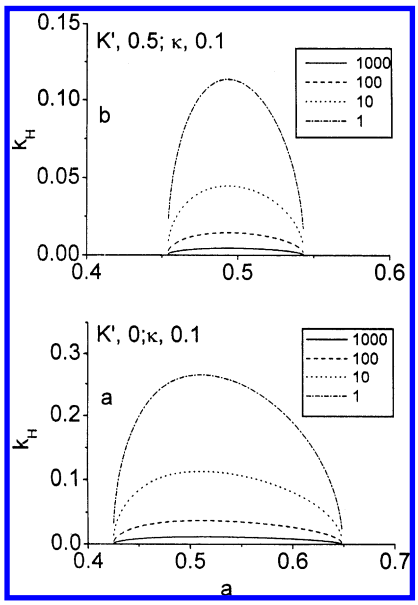

Figure 2. Hopf wavenumber (k_H) as a function of a for four different values of d; κ, 0.1; other parameters, same as Figure 1: (a) K', 0; (b) K', 0.5.

R−D experiment of glycolysis in yeast extracts, is direct evidence in support of our numerical simulation. The value predicted from another R−D model of glycolysis[20,21] is about 3 mm in length.

The wavenumber $k = 0$ (wavelength, infinitely large) should make the reaction medium perfectly homogeneous, which can be attained in a real experiment only at a very high stirring rate, where molecular diffusion has no chance to act. A decrease in stirring initiates the role of molecular diffusion as a transport process, introducing inhomogeneity from imperfect mixing.[22,23] This inhomogeneity manifests itself in the form of nonzero wavenumber modes in an unstirred R−D medium, where the wavenumber may attain its maximum value (wavelength, shortest) as decided solely by the bifurcation parameters. We have made a numerical estimate of the domain of the different nonzero wavenumber modes in the parameter space for low (2.5), moderate (10), and high (100) values of d in the absence (K, 0) and presence ($K > 0$) of the complexing reaction of the activator P.

The result is presented in Figures 3 and 4 in the form of phase diagrams in $a-\kappa$ parameter space. In the absence of any

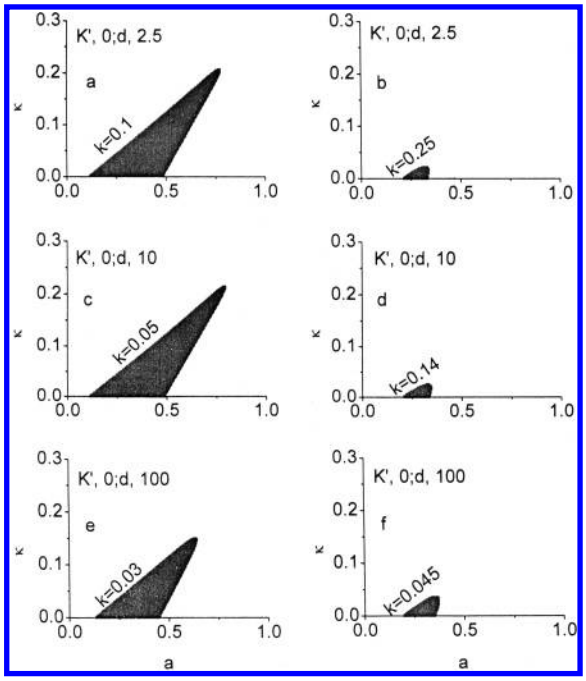

Figure 3. Phase diagrams in the $a-\kappa$ phase plane of the reversible Selkov model for $K' = 0$; other parameters, same as Figure 1: (a) d, 2.5; k, 0.1; (b) d, 2.5; k, 0.25; (c) d, 10; k, 0.05; (d) d, 10; k, 0.14; (e) d, 100; k, 0.03; (f) d, 100; k, 0.045. (Shaded areas are Hopf-wave regions for the particular wavenumbers as indicated.)

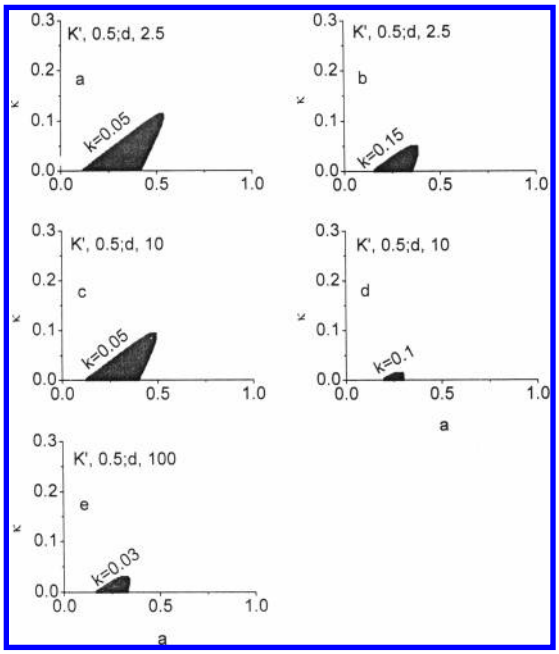

Figure 4. Phase diagrams in the $a-\kappa$ phase plane of the reversible Selkov model for $K' = 0.5$; other parameters, same as Figure 1: (a) d, 2,5; k, 0.05; (b) d, 2.5; k, 0.15; (c) d, 10; k, 0.05; (d) d, 10; k, 0.1; (e) d, 100; k, 0.03. (Shaded areas are Hopf-wave regions for the particular wavenumbers as indicated.)

complexing reaction of the activator P, Figures 3a and 3b are the phase diagrams for $d = 2.5$ for two possible extreme values of the wavenumber k. Figures 3c and 3d present the corresponding phase diagrams for $d = 10$ for two possible extreme values of the wavenumber k, and Figures 3e and 3f present the corresponding phase diagrams for $d = 100$ for two possible extreme values of the wavenumber k. In the presence of the complexing reaction with the activator P (K', 0.5), Figures 4a and 4b are the phase diagrams for $d = 2.5$ for two extreme

values of the wavenumber k. Figures 4c and 4d present the corresponding phase diagrams for $d = 10$ for two extreme values of the wavenumber k, and Figure 4e presents the phase diagram for $d = 100$ for the wavenumber $k = 0.03$. Only the phase diagrams for the two extreme values of k are presented, because those for the other intermediate values of k show similar orders, particularly the magnitude of the areas of the Hopf-wave domains.

Comparison of the phase diagrams as presented in Figures 3a to 3b, Figures 3c to 3d, and Figures 3e to 3f for low (2.5), moderate (10), and high (100) values of d, respectively, in the absence of the complexing reaction of the activator P indicates that the low values of d do help to generate large wavenumber (short wavelength) Hopf instability in our model system. Comparing the corresponding phase diagrams presented in Figures 4a to 4b, Figures 4c to 4d and Figure 4e, respectively, we obtain the same trend as that obtained in the absence of the complexing reaction presented in Figures 3a to 3b, Figures 3c to 3d, and Figures 3e to 3f, respectively. It is interesting to note that the areas of the phase diagrams in the parameter space and the corresponding maximum values of the possible wavenumber k (shortest wavelength) are reduced drastically at high values of d as well as in the presence of the complexing reaction of the activator P. This result is in agreement with that obtained in Figures 2a and 2b from k_H versus a plots in the absence and presence of the complexing reaction with the activator P, respectively.

Different higher values of d can be realized by assuming a regulatory mechanism, which is based on immobilization of the activator P in a real glycolytic experiment. Therefore, the experimental wavenumbers (wavelengths) of the Hopf waves including target patterns, spiral waves, etc. at different values of d and bifurcation parameters may be used to test the findings of the numerical predictions reported here.

This paper has reported only the Hopf-wave instability in the reversible Selkov model[17] but has not considered any kind of interaction[24−26] with space-periodic, stationary Turing patterns. Interaction and competition between these two symmetry-breaking modes is expected to generate a large variety of spatiotemporal patterns, including combinations of Turing structures and spiral waves. Our future simulations will be directed to explore these possibilities in the reversible Selkov model[17,18] of glycolytic oscillations.

References and Notes

(1) Nicolis, G.; Prigogine, I. *Self-Organization in Nonequilibrium Systems*; Wiley: New York, 1977.
(2) *Waves and Patterns in Chemical and Biological Media*; Swinney, H. L., Krinsky, V. I. Eds.; *Physica D* **1991**, *49* (1 and 2).
(3) Zhabotinsky, A. M.; Dolnik, M.; Epstein, I. R. *J. Chem. Phys.* **1995**, *103*, 10306.
(4) De Wit, A.; Lima, D.; Dewel, G.; Borckmans, P. *Phys. Rev. E* **1996**, *54*, 261.
(5) Dolnik, M.; Rovinsky, A. B.; Zhabotinsky, A. M.; Epstein, I. R. *J. Phys. Chem. A* **1999**, *103*, 38.
(6) Castets, V.; Dulos, E.; Boissonade, J.; De Kepper, P. *Phys. Rev. Lett.* **1990**, *64*, 2953.
(7) De Kepper, P.; Epstein, I.; Orban, M.; Kustin, K. *J. Phys. Chem.* **1982**, *86*, 170.
(8) Lengyel, I.; Epstein, I. *Acc. Chem. Res.* **1993**, *26*, 235.
(9) Epstein, I.; Lengyel, I. *Physica D*, **1995**, *84*, 1.
(10) Rudovics, B.; Barillot, E.; Davies, P.; Dulos, E.; Boissonade, J.; De Kepper, P. *J. Phys. Chem. A* **1999**, *103*, 1790.
(11) Lee, K.; McCormick, W.; Swinney, H.; Noszticzius, Z. *J. Chem. Phys.* **1992**, *95*, 4048.
(12) Agladze, K.; Dulos, E.; De Kepper, P. *J. Phys. Chem.* **1992**, *96*, 2400.
(13) Noszticzius, Z.; Ouyang, Q.; McCormick, W.; Swinney, H. *J. Phys. Chem.* **1992**, *96*, 6302.
(14) Lengyel, I.; Epstein, I. *Science* **1991**, *251*, 650.
(15) Lengyel, I.; Epstein, I. *Proc. Natl. Acad. Sci. U.S.A.* **1992**, *89*, 3977.
(16) Dutt, A. K., submitted for publication.
(17) (a) Richter, P.; Regmus, P.; Ross, J. *Prog. Theor. Phys.* **1981**, *66*, 385. (b) Dutt, A. K. *Chem. Phys. Lett.* **1993**, *208*, 139.
(18) Selkov, E. E. *Eur. J. Biochem.* **1968**, *4*, 79.
(19) Müller, S.; Plesser, T.; Boiteaux, A.; Hess, B. *Z. Naturforsch., C: J. Biosci.* **1985**, *40*, 588.
(20) Goldbeter, A.; Lefever, R. *Biophys. J.* **1972**, *12*, 1302.
(21) Goldbeter, A. *Proc. Natl. Acad. Sci. U.S.A.* **1973**, *70*, 3255.
(22) Epstein, I. *Nature* **1990**, *346*, 16.
(23) Dutt, A. K.; Datta, A. *J. Phys. Chem. A* **1998**, *102*, 7981.
(24) Vanag, V.; Epstein, I. *Science* **2001**, *294*, 835.
(25) Vanag, V.; Epstein, I. *Phys. Rev. Lett.* **2001**, *87*, 22830.
(26) Yang, L.;.Dolnik, M.; Zhabotinsky, A.; Epstein, I. .*J. Chem. Phys.* **2002**, *117*, 7259.